

1 *Conference Proceedings Paper*

2 Development of prediction model for storm surge hazard in the developing countries

3 **Hasibun Naher^{1,*} and Gour Chandra Paul²**

4 Published: date

5 Academic Editor: name

6 Affiliation 1: Department of Mathematics and Natural Sciences, Brac University, 66 Mohakhali, Dhaka 1212,
7 Bangladesh

8 Affiliation 2 : Department of Mathematics, University of Rajshahi, Rajshahi 6205, Bangladesh

9
10 * Correspondence: hasibun06tasauf@gmail.com; Tel.: +88-01818182462

11 **Abstract:** Bangladesh is one of the most vulnerable countries in the world with around 718000 deaths in the
12 past fifty years. This country is especially in danger for cyclones because of its locations at the
13 triangular-shaped Bay of Bengal. The scientific scenario suggests that enlarged sea surface temperature will
14 intensify cyclone movement. Tropical cyclone generates storm surge. **Storm surges severely change the coastal
15 environment, damage coastal structures, destroy forests, crops, inundate the coastline with saltwater and loss of
16 lives.** Due to overcrowding in the mainland in Bangladesh, poor and landless people live in the coast and they
17 face frequent cyclones and associated surges. They affect to have food and drinking water; in danger the
18 transmission risks of infectious diseases, such as diarrhoea, malaria, eye infections, skin diseases, etc. Some
19 problems following a cyclone usually create for their low literacy rate and poor knowledge of the environment.
20 The tangible monitoring and warning of the cyclones and associated surges should be given more priority for
21 the region.

22 The main objectives of this paper are to highlight the existing activities as the model in storm surges and related
23 areas in the Bay of Bengal. We would explain the progress of a location-specific real-time standpoint prediction
24 system for providing effective and timely surge forecasts. We would also introduce a model through numerical
25 experiments with severe cyclone April 1991 to predict the storm surges that would be used to reduce economic
26 losses and the number of death tolls during a strong storm surge in the coastal area of Bangladesh.

27
28 **Keywords:** Tropical cyclone; Bay of Bengal; storm surge; numerical modeling; coastal environment.
29

30 1. Introduction

31 Storm surges are associated with severe weather such as tropical cyclones that constitute the world's most
32 catastrophic natural disaster [1]. Among the most threatening calamities, storm surge stands out as the most
33 damaging and undoubtedly as a cause of death and ruin as massive as that of earthquake and tsunami [2]. In
34 history, low-lying deltaic regions of Bangladesh and Myanmar are heavily subjected to storm surge hazard.
35 Fortunately, in most recent storm surge cases, the death is not as high as previous since the storm surge warning
36 systems in fact worked well. However to keep our mind that storm surge can be a cause of high death rate in the
37 future while the number of residents is rising in coastal regions [3, 4]. The key components contributing to
38 calamitous surges in Bangladesh are as follows [5]:

The 3rd International Electronic Conference on Geosciences, 7 - 13 December 2020

- 39 ❖ Convergence of the Bay
- 40 ❖ High Astronomical Tides
- 41 ❖ Positive Cyclone Track
- 42 ❖ Shallow Coastal Water
- 43 ❖ Densely Populated Low-lying Island

44 Updated and accurate storm surge prediction system is required to mitigate and prevent coastal disasters. It is
 45 essential to study local allocation characteristics exclusively along with previous storm surge height in order to
 46 update the numerical forecast systems. Various ranges of motion must be investigated through numerical
 47 discrete structure of the governing equations to forecast surge in coastal area exactly. It is also indispensable to
 48 examine long-term observation data perfectly in predicting the areas that storm surges might affect with
 49 precession [6-8]. As the landward boundary is approached, substantial grid refinement is typically required to
 50 resolve important scheme and prevent energy from aliasing. In providing adequate resolution in the **near shore**
 51 region without increasing the size of the discrete problem, a numerical method must be used that permits a very
 52 high degree of grid flexibility.

53 2. Materials

54 **Model equation:** The following depth-averaged vertically integrated form of the mass conservation equation,
 55 and the x and y components of the momentum equation, respectively, are used in investigating the dynamical
 56 process in the sea [6]:

$$57 \quad \frac{\partial \xi}{\partial t} + \frac{\partial}{\partial x}[(\zeta + h)u] + \frac{\partial}{\partial y}[(\zeta + h)v] = 0, \quad (1)$$

$$58 \quad \frac{\partial u}{\partial t} + u \frac{\partial u}{\partial x} + v \frac{\partial u}{\partial y} - fv = -g \frac{\partial \xi}{\partial x} + \frac{T_x}{\rho(\xi + h)} - C_f \frac{u(u^2 + v^2)^{1/2}}{\xi + h}, \quad (2)$$

$$59 \quad \frac{\partial v}{\partial t} + u \frac{\partial v}{\partial x} + v \frac{\partial v}{\partial y} + fu = -g \frac{\partial \xi}{\partial y} + \frac{T_y}{\rho(\xi + h)} - C_f \frac{v(u^2 + v^2)^{1/2}}{\xi + h}. \quad (3)$$

60 In Eqs. (1)-(3), x and y are coordinate axes directed towards the south and east, respectively, where the origin
 61 is set at the northwest corner ($23^\circ\text{N}, 85^\circ\text{E}$) of the computational xy -plane (Fig. 1); u and v represent
 62 Reynold's averaged components of velocity in the x and y directions, respectively; $\zeta(x, y, t)$ is displaced
 63 level of the free surface of water above or below the mean sea level (MSL); $h(x, y)$ is the undisturbed water
 64 depth; $f (= 2\Omega \sin \phi)$, where Ω is the angular speed of the earth rotation about its own axis, and ϕ
 65 represents the latitude of a position of interest) is the Coriolis parameter; $g (= 9.81 \text{ m/s}^2)$ is the acceleration
 66 due to local gravity; ρ is the sea water density, assumed to be uniform; $C_f (= 0.0026)$ is the dimensionless
 67 bottom friction coefficient; T_x and T_y are the x and y components, respectively, of the wind stress acting
 68 on the sea surface.

69 The wind stress components mentioned above are derived following Ali [5] as

$$70 \quad (T_x, T_y) = \rho_a C_D (u_a^2 + v_a^2)^{1/2} (u_a, v_a). \quad (4)$$

71 To derive the components of the wind stress, wind field is required. As in [7], the wind field is generated
 72 through the following formula:

73
$$v_a = \begin{cases} V_o \sqrt{(r_a/R)^3}, & \text{for } r_a \leq R \\ V_o \sqrt{(R/r_a)^3}, & \text{for } r_a > R \end{cases} \quad (5)$$

74 In Eqs. (4) and (5), u_a and v_a stand for the x and y components of the surface wind, respectively, ρ_a is the
 75 air density, $C_D (= 0.0028)$ is the surface drag coefficient, V_0 is the maximum sustained wind at the maximum
 76 radial distance R and r_a is the distance between the cyclone centre and the point at which the wind field is
 77 desired.

78
 79 **Boundary Conditions:** The study domain has three open boundaries and one closed boundary. At the closed
 80 boundary (Costal or island boundary), the normal component of the depth averaged velocity is set to zero.
 81 Following Paul et al. [6], the western, eastern and southern open boundary conditions are, respectively, taken
 82 into account. These lead to

83
$$v + (g/h)^{1/2} \zeta = 0, \quad v - (g/h)^{1/2} \zeta = 0, \quad u - (g/h)^{1/2} \zeta = -2a(g/h)^{1/2} \sin\left(\frac{2\pi t}{T} + \varphi\right), \quad (6)$$

84 where a , T , and φ stand for, respectively, the amplitude, period, and phase of the tidal constituent under
 85 consideration.

86 Meghna River mouth is considered as open boundary and the freshwater discharge through the river is
 87 considered following Roy [7]. This leads to

88
$$u_b = u + \frac{Q}{B(h + \zeta)}, \quad (7)$$

89 where Q denotes the volume of freshwater river discharge in a unit time and B represents its width.

90 **Input:** In our study, we need several types of input. The meteorological input, namely maximum sustained
 91 wind radius, maximum sustained wind speed, and storm track information are obtained from the Bangladesh
 92 Meteorological Department (BMD) through personal communication. The time varying positions of the storm
 93 and its nature are presented in Table 2 for a better understanding. The study also needs bathymetry data which is
 94 collected from the British Admiralty Chart. Shepard interpolation is used to supply water depth at the grid
 95 points of the three schemes, as we will see later, representing water. Further, the study needs tidal constants to
 96 generate a tidal response on the area of interest, which are taken from the study due to Paul et al. [6]. Following
 97 Paul et al. [9], the freshwater discharge through the river per unit time is taken as $Q = 5100\text{kg/s}$ and the remaining
 98 parameters have been assumed to have their standard value.

99

Table 1 Time series for the positions and the nature of the April 1991 cyclone (Source: BMD)

Date (1991)	Hour (UTC)	Latitude (°N)	Longitude (°E)	Nature of the storm
26 April	1800	11.80	87.50	Cyclonic storm
27 April	0300	12.50	87.50	Cyclonic storm
27 April	0600	13.00	87.50	Cyclonic storm
27 April	0900	13.60	87.50	Severe cyclonic storm
27 April	1800	14.50	87.50	Severe cyclonic storm with hurricane core
28 April	0600	15.80	87.70	Severe cyclonic storm with hurricane core
28 April	0800	16.50	88.00	Severe cyclonic storm with hurricane core
28 April	1800	17.60	88.30	Severe cyclonic storm with hurricane core

29 April	0600	19.80	89.40	Severe cyclonic storm with hurricane core
29 April	1200	20.80	90.40	Severe cyclonic storm with hurricane core
29 April	1800	22.00	91.40	Severe cyclonic storm with hurricane core
29 April	2000	22.30	91.80	Crossing the coast near Chittagong
30 April	0000	23.00	92.40	Crossed the Bangladesh coast
30 April	0200	23.50	92.80	--

101 Maximum wind speed: 234 km h⁻¹, maximum radius of sustained wind: 50 km

102 **3. Methodology:**

103 **3.1 Numerical procedures:**

104 **3.1.1 Set-up of nested scheme:** In order to incorporate the coastal complexity with minimum cost, nested grid
 105 technique is used in this study. A high resolution fine grid model, referred to as FMS, is nested into a scheme
 106 with relatively low resolution, which is referred to as CMS. It is of interest to note here that the FMS is designed
 107 to incorporate all the major offshore islands along the coast of Bangladesh. Now to incorporate properly the
 108 land-sea interface and bottom topographic detail of the Meghna estuarine area, which is referred to as the world
 109 most vulnerable zone, a scheme with very high resolution is nested into the FMS. The innermost scheme is
 110 referred to as VFMS. To have a clear idea about the schemes, Fig. 1 and Table 1 are inserted for a better
 111 perspective. It is to be noted here that Paul et al. [6] first used the MOL to solve shallow water equations in
 112 predicting water levels due to the tide-surge interaction along the coast of Bangladesh, where they used nested
 113 grid technique without high resolution of grids. Thus, this study is an improvement on that of Paul et al. [6].

114
 115 **3.1.2 Discretization:** The aim of the study is to solve the governing equations with numerical method of lines
 116 (MOL). It is of interest to note here that the method is efficient over the standard finite difference method due
 117 to having some benefits, especially, in computational cost, stability criterion, and simplicity in solving partial
 118 differential equations. Thus, in this regard, the equations and the boundary conditions are discretized only for
 119 spatial derivatives/variables by means of semi-implicit three point central finite difference technique. We
 120 consider the discrete points in the xy-plane, by defining $x_i = (i-1)\Delta x$, $i=1,2,3,\dots,M$ (even), $y_j = (j-1)\Delta y$,
 121 $j=1,2,3,\dots,N$ (odd).

122 If any dependent variable $\xi(x, y, t)$ at a grid point (x_i, y_j) at time t_k is represented by $\xi(x_i, y_j, t_k) = \xi_{i,j}^k$,

123 then with the aid of the notations $0.5(\xi_{i+1,j}^k + \xi_{i-1,j}^k) = \overline{\xi_{i,j}^k}^x$, $0.5(\xi_{i,j+1}^k + \xi_{i,j-1}^k) = \overline{\xi_{i,j}^k}^y$, and

124 $0.25(\xi_{i+1,j}^k + \xi_{i-1,j}^k + \xi_{i,j+1}^k + \xi_{i,j-1}^k) = \overline{\xi_{i,j}^k}^{xy}$, we have discretized our equations of interest as follows.

125 For every grid point (x_i, y_j) , where $i=2,4,6,\dots,M-2$ and $j=3,5,7,\dots,N-2$, Eq. (1) can be written as

126
$$\left(\frac{\partial \zeta}{\partial t}\right)_{i,j} = f_1(\zeta_{l,m}^k, u_{l,m}^k, v_{l,m}^k, h_{l,m}) = CR1 + CR2, \quad (8)$$

127 where $l=i-1, i, i+1; m=j-1, j, j+1$;

128
$$CR1 = -\frac{(\overline{\zeta_{i+1,j}^k}^x + h_{i+1,j})u_{i+1,j}^k - (\overline{\zeta_{i-1,j}^k}^x + h_{i-1,j})u_{i-1,j}^k}{2\Delta x}, \quad CR2 = -\frac{(\overline{\zeta_{i,j+1}^k}^y + h_{i,j+1})v_{i,j+1}^k - (\overline{\zeta_{i,j-1}^k}^y + h_{i,j-1})v_{i,j-1}^k}{2\Delta y}.$$

129 Again, for every point (x_i, y_j) , where $i = 3, 5, 7, \dots, M-1$ and $j = 3, 5, 7, \dots, N-2$, Eq. (2) can be written as

$$130 \left(\frac{\partial u}{\partial t} \right)_{i,j} = f_2(\xi_{l,m}^{k+1}, u_{l,m}^k, v_{l,m}^k, h_{l,m}) = UR1 + UR2 + UR3 + UR4 + UR5 + UR6, \quad (9)$$

131 where $l = i-2, i-1, i, i+1, i+2; m = j-2, j-1, j, j+1, j+2$;

$$132 UR1 = - \begin{cases} u_{i,j}^k \frac{u_{i+2,j}^k - u_{i-2,j}^k}{4\Delta x}, & \text{for } i \neq m-1 \\ u_{i,j}^k \frac{0.5(3u_{i,j}^k - u_{i-2,j}^k) - u_{i-2,j}^k}{4\Delta x}, & \text{for } i = m-1 \end{cases}, \quad UR2 = -v_{i,j}^{k-xy} \frac{u_{i,j+1}^k - u_{i,j-1}^k}{2\Delta y}, \quad UR3 = f_{i,j} \overline{v_{i,j}^{k-xy}},$$

$$133 UR4 = -g \frac{\zeta_{i+1,j}^{k+1} - \zeta_{i-1,j}^{k+1}}{2\Delta x}, \quad UR5 = \frac{T_x}{\rho(\zeta_{i,j}^{k+1} + h_{i,j})}, \quad UR6 = -\frac{C_f u_{i,j}^k}{\zeta_{i,j}^{k+1} + h_{i,j}} \left[(u_{i,j}^k)^2 + (\overline{v_{i,j}^{k-xy}})^2 \right]^{1/2},$$

134 Finally, for every grid point (x_i, y_j) , where $i = 2, 4, 6, \dots, M-2$ and $j = 2, 4, 6, \dots, N-1$, Eq. (3) can be
135 written as

$$136 \left(\frac{\partial v}{\partial t} \right)_{i,j} = f_3(\xi_{l,m}^{k+1}, u_{l,m}^k, v_{l,m}^k, h_{l,m}) = VR1 + VR2 + VR3 + VR4 + VR5 + VR6, \quad (10)$$

137 where $l = i-2, i-1, i, i+1, i+2; m = j-2, j-1, j, j+1, j+2$;

$$138 VR1 = - \begin{cases} u_{i,j}^{k-xy} \frac{v_{i+1,j}^k - v_{i-1,j}^k}{2\Delta x}, & \text{for } i \neq 2 \\ u_{i,j}^{k-xy} \frac{v_{i+1,j}^k - 0.5(3v_{i,j}^k - v_{i+2,j}^k)}{2\Delta x}, & \text{for } i = 2 \end{cases}$$

$$139 VR2 = - \begin{cases} v_{i,j}^k \frac{v_{i,j+2}^k - v_{i,j-2}^k}{4\Delta y}, & \text{for } j \neq 2, j \neq n-1 \\ v_{i,j}^k \frac{v_{i,j+2}^k - 0.5(3v_{i,j}^k - v_{i,j+2}^k)}{4\Delta y}, & \text{for } j = 2 \\ v_{i,j}^k \frac{0.5(3v_{i,j}^k - v_{i,j-2}^k) - v_{i,j-2}^k}{4\Delta y}, & \text{for } j = n-1 \end{cases}, \quad VR3 = -f_{i,j} \overline{u_{i,j}^{k-xy}}, \quad VR4 = -g \frac{\zeta_{i,j+1}^{k+1} - \zeta_{i,j-1}^{k+1}}{2\Delta y},$$

$$140 VR5 = \frac{T_y}{\rho(\zeta_{i,j}^{k+1} + h_{i,j})}, \quad VR6 = -\frac{C_f v_{i,j}^k}{\zeta_{i,j}^{k+1} + h_{i,j}} \left[(\overline{u_{i,j}^{k-xy}})^2 + (v_{i,j}^k)^2 \right]^{1/2}.$$

141
142 The boundary conditions specified by Eqs. (6), the elevations at $j = 1$ (eastern boundary), $j = N$ (western
143 boundary, and $i = M$ (southern boundary) are computed in the following manner, respectively:

$$144 \zeta_{i,1}^{k+1} = -\zeta_{i,3}^{k+1} - 2\sqrt{(h_{i,2}/g)} V_{i,2}^k, \quad (11)$$

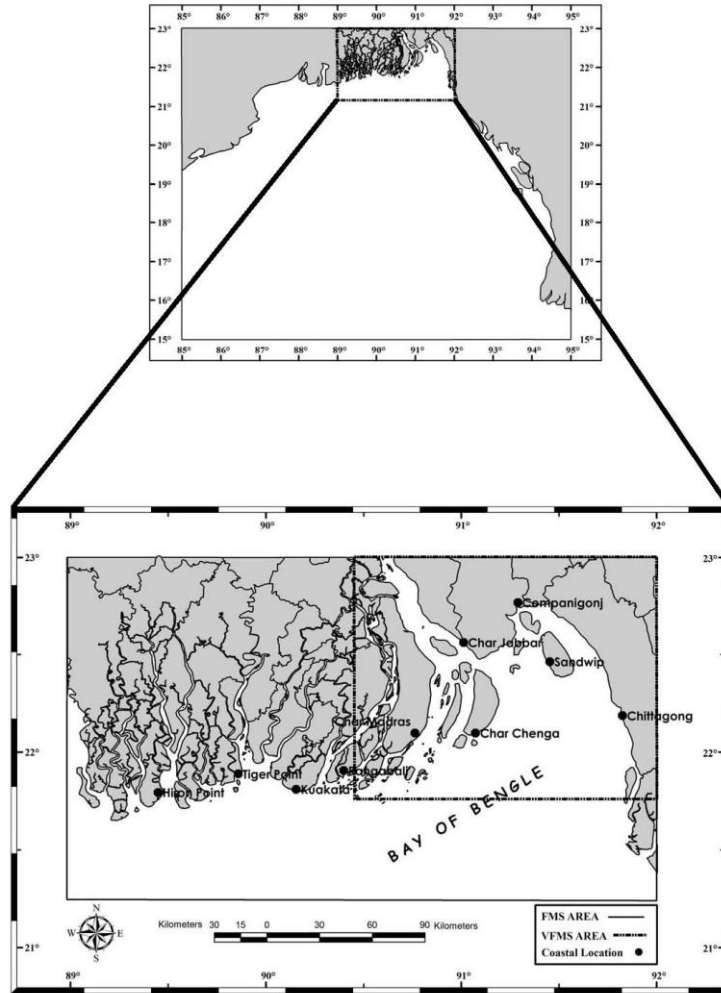
$$145 \zeta_{i,N}^{k+1} = -\zeta_{i,N-2}^{k+1} + 2\sqrt{(h_{i,N-1}/g)} V_{i,N-1}^k, \quad (12)$$

$$146 \zeta_{M,j}^{k+1} = -\zeta_{M-2,j}^{k+1} + 2\sqrt{(h_{M-1,j}/g)} U_{M-1,j}^k + 4a \sin(2\pi k\Delta t/T + \varphi), \quad (13)$$

147 where $i = 2, 4, 6, \dots, M-2$ and $j = 1, 3, 5, \dots, N$.

148 The freshwater Meghna River discharge is incorporated through Eq. (7), where the velocity component U_b is
 149 calculated at $(1, j)$, $j = 7, 9, 11, \dots, 19$ in the following manner:

150
$$(U_b)_{1,j}^{k+1} = (U_b)_{3,j}^{k+1} + \frac{Q}{(\zeta_{1,j}^{k+1} + h_{1,j})B} \quad (14)$$



151
 152 **Fig. 1** Domains of the three schemes CMS, FMS and VFMS and actual coastal and island boundaries along with
 153 ten representative locations at which computed results are presented (after Paul et al. [9])

154 **Table 2** Domains, grid resolutions and number of grid points of different schemes (after Paul et al. [9])

Model	Domain extent	Grid resolution along x-axis	Grid resolution along y-axis	Number of grid points
CMS	15° – 23° N and 85° – 95° E	15.08 km	17.52 km	60 × 61
FMS	21.25° and 89° – 92° E	2.15 km	3.29 km	92 × 95
VFMS	21.77° – 23° N and 90.40° - 92° E	720.73 m	1142.39 m	190 × 145

155

156 **3.1.3. Working procedure and model run:** Discretized form of Eqs. (8)-(10) are available in [6]. However,
 157 briefly they are inserted here for a better understanding. First Eq. (8) is solved with RK(4,4) method for the
 158 elevation ζ at the internal (even, odd) grid points representing water of the CMS. Discretized BCs given by
 159 Eqs. (11)-(13) are then used to estimate ζ at the boundary (even, odd) grid points. An interpolation is then
 160 adopted to obtain ζ at the leftover grid points representing water and the land-sea interface. The wind field is
 161 then generated using Eqs. (4) and (5). Then Eq. (9) is used for estimating u at the interior (odd, odd) grid
 162 points representing water by inserting the parametric values involved and finally v is evaluated in a similar
 163 fashion at the interior (even, even) grid points solving Eq. (10). After computing ζ , u , and v in the CMS,
 164 the scheme is coupled with the FMS following a process found in [6] to have the boundary values from the CMS
 165 to run the FMS. In a similar manner, the VFMS is run with the boundary information from the FMS. Along the
 166 northern open boundary segment, U_b is taken into account for the VFMS using Eq. (14). This process is
 167 repeated over time providing the updated values of ζ , u , and v as initial conditions for computing WLs
 168 (ζ) owing to tide, surge, and nonlinear interaction of tide and surge. For computing tide, surge, and total water
 169 levels (water levels due to tide-surge interaction) all the models, namely tide, surge, and tide-surge interaction
 170 were run considering the time step as $\Delta t = 60$ s to ensure Courant-Friedrichs-Lewy (CFL) stability criterion. It
 171 is noteworthy that our model can run individually and simultaneously. First tide model was run from the cold
 172 start ($\zeta = 0, u = 0, v = 0$ at $t = 0$) to get water levels with respect to the mean sea levels (MSL) considering the
 173 effect of M_2 tidal constituent along the southern open boundary of the CMS in the absence of meteorological
 174 forcing. A stable tidal oscillation was obtained after 4 tidal cycles of integration that provided the profile of the
 175 sea surface if the cyclone is not taken into account. In getting the pure surge level, the surge model (in absence
 176 of astronomical tide) was also run from the cold start. In achieving total WLs (due to the dynamic interaction of
 177 tide and surge), the tide model was run first. After having a stable tidal regime, the surge model was then made
 178 run over it.

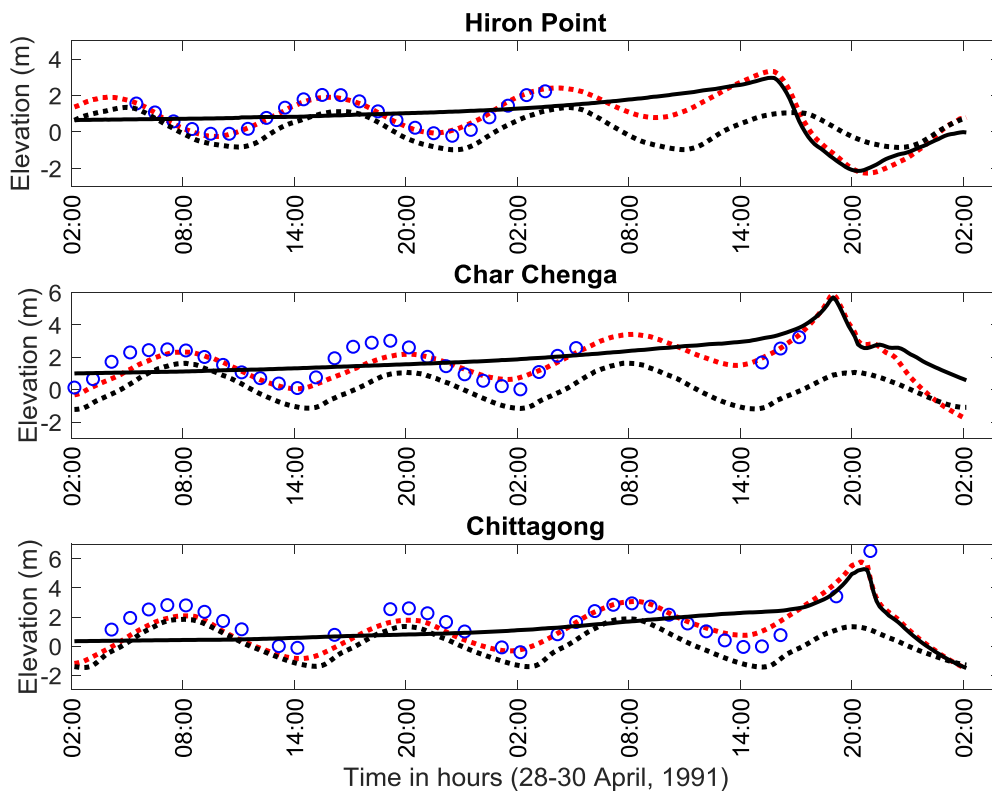
179 **4. Results and discussion:** Water levels due to tide, surge and their interaction are calculated at the stations
 180 shown in Fig. 1. But for the sake of brevity, the peak water levels due to surge and interaction of tide and surge
 181 are presented in Table 3 and computed time series of water levels due to the tide, surge, and the interaction of
 182 tide and surge are presented in Fig. 2 with observed data. It is seen from Table 3 that our computed peak surge
 183 levels (water levels due to meteorological forcing only) along the region of interest vary between 2.97-6.51 m
 184 with 5.29 m at Chittagong. Paul et al. [6] predicted 3.52-6.70 m surge along the coast of Bangladesh. Further,
 185 according to BMD, the peak surge at Chittagong at the time of landfall was 5.50 m. Thus, our computed surge
 186 level agree well with the reported data by BMD at Chittagong and the simulated surge levels by Paul et al. [6].
 187 Again, our computed peak total water levels were found to vary between 3.86 m (Kuakata) and 7.28 m
 188 (Companigonj), which agree fairly well with the results obtained in Paul et al. [6] (see Table 3).

189 Our computed time series of water levels with respect to the MSL due to tide, surge and the interaction of tide
 190 and surge associated with the storm April 1991 at Hiron Point, Char Chenga (Hatiya), and Chittagong are
 191 displayed in Fig. 2. The corresponding observed data collected from Bangladesh Inland Water Transport
 192 Authority (BIWTA) are also presented in Fig. 2. It is seen from Fig. 2 that when the surge is away from the
 193 coast, then tide dominates the surge level, whether the opposite characteristics can be found when the surge is
 194 nearer to the coast as is expected. However, it is perceived from Fig. 2 that our computed water levels due to the
 195 interaction of tide and surge are in good agreement with the data obtained from BIWTA.

196
197

Table 3. Computed peak water levels simulated by the present study with respect to the mean sea level (MSL) and those obtained in [6]

Coastal location	Present study		Study due to Paul et al. [6]	
	Simulated maximum surge level (m)	Simulated maximum total water level (m)	Maximum surge level (m)	Maximum total water level (m)
Hiron point	2.97	3.32	3.92	4.01
Tiger point	4.11	4.51	4.21	4.57
Kuakata	3.25	3.82	3.52	3.86
Char Chenga	5.70	5.89	5.11	5.81
Char Jobbar	6.12	6.33	6.19	6.35
Companigonj	6.51	6.30	6.70	7.28
Sandwip	5.40	5.71	5.24	5.63
Chittagong	5.29	5.79	5.17	6.26



198
199
200
201
202
203
204
205

Figure. 2 Computed water levels with respect to the mean sea level due to tide, surge, and their interaction with observed data at (a) Hiron Point, (b) Char Chenga and (c) Chittagong. In each subplot, a black solid curve represents the configuration for tide, black dotted curve that for tide, red dotted curve for tide-surge interaction, and a circle represents observed data.

For validation of our simulated results, the root mean square analysis is carried out between the results attained in the study and observed data from BIWTA. The results came out in this regard are presented in Table 4. The

206 root mean square error (RMSE) values obtained in this regard due to Paul et al. [9] are also presented in the
 207 same table for comparison. It is seen from Table 4 that the results attained by the study are considerable and
 208 comparable with those presented in [9].

209 **Table 4** Estimated RMSEs in metre. The errors have been estimated between computed and observed water
 210 levels from 02.00 UTC of April 28 to 02.00 UTC of April 30 for the storm April 1991. The observed data were
 211 obtained from BIWTA
 212

Costal station	Estimated by the model	Estimated by the model due to Paul et al. [9]
Chittagong	0.78	0.73
Char Chenga	0.55	0.58
Hiron Point	0.18	0.16

213
 214 **5. Conclusions:** In this study, the MOL in coordination with the RK (4,4) method is used to solve vertically
 215 integrated shallow water equations in Cartesian coordinates for simulating water levels along the coast of
 216 Bangladesh. The water levels due to the non-linear interaction of tide and surge associated with the cyclone
 217 April 1991 are found to be in reasonable agreement with observed data from BIWTA on the basis of RMSE
 218 values. The outcome of this study thus can be utilized in practical forecasting.

219 **Acknowledgements:** Authors would like to articulate their heartfelt thanks to the Department of Mathematics
 220 and Natural Sciences, Brac University, Dhaka, Bangladesh for providing suitable research facilities.
 221 Moreover, authors are pleasure to express their genuine appreciation to the anonymous referees for their
 222 significant comments and suggestions.

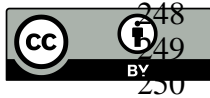
223 **Authors Contributions:** H. N and G. P conceived and designed the experiments and also analyzed the data. H.
 224 N and G. P completed the writing of the manuscript by sharing their knowledge and ideas and polished the
 225 paper through double checking.

226 **Conflict of Interest:** The authors declare no conflict of interest.

227 **References**

228 1. Dube, S. K., Rao, A. D., Sinha, P. C., Murty, T. S., & Bahulayan, N. Storm surge in the Bay of Bengal and
 229 Arabian Sea the problem and its prediction. *Mausam*, 1997, 48(2), 283-304.
 230 2. Li, J., & Nie, B. Storm surge prediction: present status and future challenges. *Procedia IUTAM*, 2017, 25,
 231 3-9.
 232 3. Kohno, N., Dube, S. K., Entel, M., Fakhruddin, S. H. M., Greenslade, D., Leroux, M. D., & Thuy, N. B.
 233 Recent progress in storm surge forecasting. *Tropical Cyclone Research and Review*, 2018, 7(2), 128-139.
 234 4. Lynch, D. R. "Progress in hydrodynamic modeling, review of U.S. contributions, 1979-1982." *Rev.*
 235 *Geophys. Space Phys.*, 1983, 21(3), 741-754.
 236 5. ALI, A. Storm surges in the Bay of Bengal and some related problems. Ph.D., Thesis, University of
 237 Reading, England, 1979, pp 227.

- 238 6. Paul, G. C., Ismail, A. I. M., and Karim, M. F. Implementation of method of lines to predict water levels due
239 to a storm along the coastal region of Bangladesh. *J. Oceanography.*, 2014, 70 (3):199–210.
- 240 7. Roy, G. D. Estimation of expected maximum possible water level along the Meghna estuary using a tide
241 and surge interaction model. *Environ. Int.*, 1995, 21(5):671–677.
- 242 8. Naher, H., & Paul, G. C. Further Development of Forecasting Model for Storm Surge Hazard along the
243 Coast of Bangladesh. *American Journal of Environmental Protection*, 2019, 7(2), 52-55.
- 244 9. Paul, G.C., Ismail, A.I.M, Rahman, A., Karim M.F. & Hoque, A. Development of tide–surge
245 interaction model for the coastal region of Bangladesh. *Estuaries and Coasts*, 2016, 39(6),1582–
246 1599.
- 247



© 2020 by the authors; licensee MDPI, Basel, Switzerland. This article is an open access article distributed under the terms and conditions of the Creative Commons by Attribution (CC-BY) license (<http://creativecommons.org/licenses/by/4.0/>).